SANDIA REPORT
SAND99–0999
Unlimited Release
Printed May 1999

Integrated Fuel-Coolant Interaction (IFCI 7.0) Code User's Manual

M. F. Young

Prepared by
Sandia National Laboratories
Albuquerque, New Mexico 87185 and Livermore, California 94550

Sandia is a multiprogram laboratory operated by Sandia Corporation, a Lockheed Martin Company, for the United States Department of Energy under Contract DE-AC04-94AL85000.

Sandia National Laboratories

Issued by Sandia National Laboratories, operated for the United States Department of Energy by Sandia Corporation.

Available to DOE and DOE contractors from
Office of Scientific and Technical Information
P.O. Box 62
Oak Ridge, TN 37831

Prices available from (703) 605-6000
Web site: http://www.ntis.gov/ordering.htm

Available to the public from
National Technical Information Service
U.S. Department of Commerce
5285 Port Royal Rd
Springfield, VA 22161

NTIS price codes
Printed copy: A05
Microfiche copy: A01

DISCLAIMER

Portions of this document may be illegible in electronic image products. Images are produced from the best available original document.

SAND99-0999
Unlimited Release
Printed May 1999

Integrated Fuel-Coolant Interaction (IFCI 7.0) Code User's Manual

M. F. Young
Modeling and Analysis Department
Sandia National Laboratories
P.O. Box 5800
Albuquerque, NM 87185-0739

Report prepared for the
U.S. Nuclear Regulatory Commission
Office of Nuclear Regulatory Research

Abstract

The integrated fuel-coolant interaction (IFCI) computer code is being developed at Sandia National Laboratories to investigate the fuel-coolant interaction (FCI) problem at large scale using a two-dimensional, three-field hydrodynamic framework and physically based models. IFCI will be capable of treating all major FCI processes in an integrated manner. This document is a description of IFCI 7.0. The user's manual describes the hydrodynamic method and physical models used in IFCI 7.0. Appendix A is an input manual provided for the creation of working decks.

Contents

Figures

Tables

Acknowledgments

The author of this manual would like to thank several members of the Sandia National Laboratories staff for their assistance in the review and preparation of this document, particularly A. W. Reed and M. Pilch. Gratitude is also expressed to John Murphy and Michael Corradini for their work with the code and documentation. Their insight has proven invaluable. The U.S. Nuclear Regulatory Commission, Office of Regulatory Research is acknowledged for their sponsorship of this work, and other fuel-coolant interaction research. Finally, the author wishes to thank Dr. Chester Gingrich, USNRC, for his technical guidance of this program.

Nomenclature

A	=	cell-centered flow area (m^2)
Ar	=	radial cell flow area (m^2)
Av	=	interfacial area per unit volume (m^2/m^3)
Az	=	axial cell flow area (m^2)
C	=	drag coefficient ($Pa\text{-}s^2/m^3$), or specific heat capacity J/kg-K
C_v	=	liquid specific heat at constant volume (J/kg-K)
C_p	=	liquid specific heat at constant pressure (J/kg-K)
D	=	drop diameter (m)
D_{AB}	=	binary diffusion coefficient, m^2/s
H	=	enthalpy at saturation (J/kg)
H_{lg}	=	latent heat of evaporation (J/kg)
M_v	=	molecular weight of vapor (steam) (kg/kmol)
N	=	number of primary fragments
P	=	pressure (Pa)
Q	=	energy transfer term (W/m^3)
T	=	temperature (K)
T^+	=	dimensionless breakup time = $v_r t/D\varepsilon^{1/2}$
a	=	adiabatic sound speed (m/s)
c	=	concentration of steam ($kmol/m^3$)
g	=	gravitational acceleration (m/s^2)
h	=	heat transfer coefficient ($W/m^2\text{-}K$), or enthalpy (J/kg)
k	=	thermal conductivity (W/m-K)
t	=	time (s)
u or e	=	internal energy (J/kg)
v	=	velocity (m/s)
$\vec{v}$	=	velocity vector (m/s)
Γ	=	mass transfer rate ($kg/m^3\text{-}s$)
Γe	=	entrainment surface area generation rate ($m^2/m^3\text{-}s$)
Γp	=	primary surface area generation rate ($m^2/m^3\text{-}s$)
α	=	volume fraction
β	=	thermal expansion coefficient (K^{-1})
ε	=	density ratio = ρ_∞/ρ_d
ρ	=	density (kg/m^3)
σ	=	surface tension (Pa-m), or Stefan-Boltzmann constant ($W/m^2\text{-}K^4$)
μ	=	dynamic viscosity (kg/m-s)
υ	=	kinematic viscosity (m^2/s)
ΔT_W	=	$T_3 - T_s$
ΔT_{sub}	=	$T_{sat} - T_2$
ΔT_v	=	$T_{sat} - T_1$
Nu	=	Nusselt number, hD/k
Pr	=	Prandtl number = $C_p \mu/k$
Re	=	Reynolds number = vD/υ
We	=	Weber number = $\rho v^2 D/\sigma$

Subscripts

1-3	=	fields 1 through 3 (vapor, water, and melt, respectively)
c	=	critical
d	=	discrete
f	=	continuous fluid
fc	=	forced convection
g	=	gas
i	=	interface
j,k	=	fields 1 - 3
l	=	liquid water
m	=	melt
nat	=	natural convection
nc	=	natural convection
p	=	primary
r	=	radial direction or relative
rad	=	radiation
s	=	structure or saturation
sat	=	saturation
sub	=	subcooled
v	=	vapor (steam)
w	=	wall or structure or melt
z	=	axial direction
∞	=	bulk fluid

Superscripts:

c	=	convective
$\bullet$	=	value at end of EOS table range

1. INTRODUCTION

The integrated fuel-coolant interaction code (IFCI) is a best-estimate computer program for analysis of phenomena related to mixing of molten nuclear reactor core material with reactor coolant (water). The latest version of the code, IFCI 7.0, has been designed for analysis of small- and intermediate-scale experiments in order to gain insight into the physics (including scaling effects) of molten fuel-coolant interactions (FCIs), and to assess and validate the code's methods, models, and correlations.

IFCI is under development at Sandia National Laboratories (SNL) and is sponsored by the U.S. Nuclear Regulatory Commission, Office of Nuclear Regulatory Research (USNRC/RES).

This document describes the use of the IFCI code (IFCI 7.0). It consists of a brief description of major models, correlations, and pertinent equations in IFCI 7.0, and an input description. It also identifies limitations of the IFCI models. The main reference for the IFCI models and correlations is the IFCI 7.0 Models and Correlations Report (Young et al. 1998). The input description addresses all input parameters and files, and discusses the impact of certain key parameters on results. Users may also refer to the IFCI 6.0 Validation and Assessment Report (Reed et al. 1995) .

1.1 The IFCI Code

The IFCI computer code was developed to investigate FCIs in as mechanistic a manner as possible. The code is intended to address all aspects of FCI phenomena, including coarse fragmentation and mixing of molten material with water, triggering, propagation and fine fragmentation, and expansion of the melt-water system. The ultimate objective of the code is to predict rates of steam generation, melt fragmentation and dispersion, shock wave generation and propagation, and system loading for explosive and nonexplosive FCIs. The intent is to study and assess FCI scenarios for nuclear reactors and other industrial applications.

1.2 Existing Documentation

Young (1987) and Dosanjh (1989) describe an early version of the IFCI code. Much of the material in these two documents on IFCI's surface area transport logic, dynamic fragmentation model, and equation-of-state package is still current. Young (1990) describes a recent code version that includes a melt surface entrainment model and a melt surface tracking algorithm. All three references describe results of IFCI runs that model a generic version of an intermediate-scale FCI pouring-mode experiment in the fully instrumented test series (FITS) (Mitchell et al. 1981; Corradini 1981a; Marshall 1988). These IFCI runs served three main purposes: (1) to demonstrate that the code architecture is essentially complete and functional; (2) to provide an early qualitative assessment of the operability of the underlying models and constitutive relations, and; (3) to improve perspective on the needs for and priorities of further model development and experimental data.

Further documentation is provided by the IFCI 7.0 Models and Correlations Report (Young et al. 1998) and the IFCI 6.0 Validation and Assessment Report (Reed et al. 1995), which describes the results of IFCI calculations of MIXA6, MAGICO, and KROTOS experiments.

1.3 Scope of Report

This report contains brief descriptions of the hydrodynamic field equations and closure relations, and the models used to describe FCI phenomena, notably models for dynamic fragmentation and surface area transport, and melt oxidation. Parametric detonation/fine-fragmentation models have also been implemented; at present, these models have been incorporated into IFCI but are not fully validated.

1.4 The Fuel-Coolant Interaction Event

It is generally agreed that the FCI process can be roughly divided into four phases: the initial coarse mixing phase, the trigger phase, the detonating propagation phase, and the hydrodynamic expansion phase. These four phases are useful conceptually, although in reality they may all be occurring simultaneously in different spatial locations in the melt-coolant mixture region. In addition to the four phases, there are also different contact modes that must be considered: the pouring mode, in which a mass of molten material is dropped into a pool of coolant; jet mixing, where a jet of melt is injected into coolant; and the stratified mode, where the melt is in a pool or layer, covered by a layer of coolant.

Coarse mixing is characterized by entry of molten material (melt) into a coolant (water) with accompanying vapor generation, intermixing of the melt, water, and vapor, and breakup of the melt into smaller diameter drops (smaller meaning on the order of 0.1-10 cm); this phase occurs on a time scale of 0.1-1.0 s. During this phase, the melt and water are insulated from one another by a vapor film, which serves to maintain the fuel temperature close to its initial value throughout coarse mixing. Breakup of the melt is thought to be governed by hydrodynamic instabilities, notably the Rayleigh-Taylor and Kelvin-Helmholtz instabilities. These breakup processes are driven by relative velocity differences or accelerations between the melt and the water/steam interface.

Triggering occurs when some local disturbance collapses the vapor films around the melt. This collapse allows direct water-melt contact or near contact, high heat transfer rates to the water, and high relative velocities in the vicinity of the trigger. If the triggering event is sufficiently strong and conditions in the mixture are favorable, the mixture may enter a detonating propagation phase. Triggering is not well understood, but is typically observed to occur quickly, on a time scale of around 100 μs, and is often initiated by contact of the melt with a solid surface (Young 1987; Kim 1985; Corradini 1981b; Kim and Corradini 1988).

The explosive propagation phase is characterized by a "reaction zone," which propagates through the mixture region. Within this reaction zone, the coarsely mixed melt is rapidly fragmented into particles in the 10-100 μm size, with accompanying rapid increase in melt surface area, release of heat to the water, and generation of shock waves. It should be noted that liberation of chemical energy is not accounted for at this time. Typical experimentally observed propagation speeds are in the 50-500 m/s range. (Mitchell et al. 1981; Corradini 1981a) The same hydrodynamic instabilities that are present during coarse mixing could also be responsible for the rapid fine fragmentation occurring during propagation, although other mechanisms may also be operative, for instance, jet penetration of the melt by the water (Marshall 1988) or shockwave—induced fragmentation.

In the expansion phase, the expanding steam-water-melt mixture converts thermal energy into work on the surroundings. This phase has been treated in detail by various researchers (Swenson and Corradini 1981; Stevenson 1980).

1.5 Other FCI Modeling

Past research on FCI phenomena has been both experimental and theoretical in nature, but has not totally succeeded in resolving questions on FCI effects at large scale. In general, most of this research has been directed to answering questions of reactor safety. Separate effects and integrated experiments have been performed at small and intermediate scales to investigate many FCI phenomena. These experiments have provided much useful information, but must be much smaller than actual reactor or industrial scales. FCIs have demonstrated scale dependence in past experiments, for instance, the "pint theory" (Mitchell et al. 1981) lower limit on the amount of melt necessary for an FCI, and there are very likely other scale-dependent processes in FCIs that are unknown at this time, making the extrapolation of experimental data to industrial scale very uncertain. On the theoretical side, lack of data on basic FCI phenomena makes choosing the correct model from among competing models very difficult; without an accurate model of the physical phenomena occurring during an FCI, the experimental results cannot be confidently extended to large scale.

Early models and correlations tended to be parametric and address only isolated aspects of FCIs. As more knowledge of FCIs was gained, models evolved to include more physics. Simultaneously, advances in computational hydrodynamics allowed incorporation of the more refined models in a suitable hydrocode framework, allowing more aspects of the FCI to be treated simultaneously in an integrated fashion.

These modeling efforts with hydrocodes have also evolved from simple models and one-dimensional, single—field hydrocodes toward more physical models and two-dimensional, multifield hydrocodes. This evolution has taken place both as the limitations of early modeling efforts have been recognized and as more advanced computational hydrodynamic techniques have become available.

Recent FCI modeling efforts have generally been aimed at either the coarse mixing phase or the detonation phase. Examples of coarse mixing calculations are those done by Bankoff and Hadid (1984), Abolfadl and Theofanous (1987), Thyagaraja and Fletcher (1986), and Chu and Corradini (1989), all for mixing in the lower plenum of a power reactor. Examples of propagation calculations are those of Carachalios et al. (1983), Medhekar et al. (1988), and Fletcher and Thyagaraja (1989). The above efforts generally have made simplifying assumptions, either in the hydrodynamic model or in the models of FCI phenomena, to make the problem more tractable. Several of the coarse mixing calculations, for instance, use a constant initial particle size (Bankoff and Hadid 1984; Abolfadl and Theofanous 1987; Thyagaraja and Fletcher 1986), an assumption that incorrectly predicts early steam generation rates and consequent early separation of melt and coolant. The propagation calculations mentioned above are one-dimensional.

2. IFCI OVERVIEW

Before describing the details of IFCI, it will be helpful to have a general understanding of the code and how it operates. Section 2 provides a general description of the IFCI code and its structure, and a brief description of IFCI's inputs and outputs.

2.1 General Description

The current state of knowledge about the physical processes occurring in FCIs, characteristics of existing hydrocodes, and the necessity of calculating FCIs in a reactor safety context were all considerations in the original design of IFCI. IFCI 7.0 has been modified to provide useful insight and a usable analysis tool for the study of FCIs.

Because of the radically different time scales associated with the different phases of an FCI, an implicit numerical hydrodynamics method is desirable for its ability to exceed the Courant limit (Roache 1972), thereby reducing computation time. The presence of at least three separate material fields in the FCI problem (water, vapor, and molten fuel), all at different temperatures and moving at different velocities, also suggested the use of a multifield method. The presence of shock waves during the propagation phase requires use of a compressible hydrodynamic method.

The Stability-Enhancing Two-Step (SETS) method (Mahaffy 1982; Dearing 1985) was chosen as the basis of an appropriate hydrodynamic method that satisfied the above criteria. This selection was originally motivated by the existence of MELPROG/MOD1 (Dosanjh 1989; Kelly 1985), a severe reactor accident code using the SETS method, which features a two-dimensional, four-field fluids compressible hydrodynamics module with many necessary models already incorporated. IFCI has been stripped of the nonessential MELPROG/MOD1 modules, but retains some vestiges of the original input, as will be seen in the input description.

MELPROG/MOD1 was designed to calculate the events occurring during a hypothetical core meltdown accident in a light-water reactor (LWR). This code already includes a phase change model, a sophisticated heat-transfer model with complete boiling curve, an equation-of-state for steam and water, a flow regime map for both vertical and horizontal flow, and models for both interphase and field-structure drag. As such, MELPROG/MOD1 could be used as the basis for IFCI, with the addition of models for FCI phenomena not covered by MELPROG/MOD1.

IFCI 7.0 consists of several modules, divided according to responsibility for calculating different physical processes, which respectively handle fluids transport, convection, boiling heat transfer, etc. Output data are available as printed output, and a binary graphics output file.

IFCI 7.0 provides a two-dimensional, r-z geometry, three-field hydrodynamics model whose fields consist of vapor (steam), water, and melt (in IFCI, these are referred to as fields 1, 2, and 3 respectively). Versions of IFCI previous to 7.0 contained a fourth field, solid debris, which was not used. A "field," in the context of the SETS method, means a set of momentum, mass continuity, and energy equations; a separate set of these equations is solved for each "field." Mass, energy, and momentum transfer between fields is represented by coupling terms in these equation sets.

IFCI is based on a two-dimensional, three-field implementation of the SETS hydrodynamic method. However, the IFCI solution method uses a conservative form of the momentum equation rather than the nonconservative form used in the original SETS method. Use of a multifield method with separate mass, momentum, and energy equations for each field allows slip between the various materials (vapor, liquid coolant, and liquid melt), and a different temperature for each material. IFCI uses an equation of state for water and steam obtained by fits to the steam tables (Los Alamos Safety Code Development Group, 1986) and a stiff gas equation of state for the melt. The constitutive relations required for the interfield coupling terms (heat transfer, momentum exchange, and phase change) include a bulk boiling model, a subcooled surface boiling model, a three-field flow regime map, and adaptations of standard heat transfer and momentum transfer correlations.

Additional models are included which are necessary to calculate phenomena that occur in FCIs. These are (1) a dynamic fragmentation model, which calculates the breakup, or change in effective diameter, of the melt based on local hydrodynamic conditions (densities and velocities), coupled with (2) a convection equation for melt surface area per unit volume; (3) a trigger model to simulate a local explosion in a melt-water-steam mixture; and (4) a detonation-fine fragmentation model to calculate the rapid fragmentation and steam generation in a propagating reaction zone. It appears, based on current understanding of FCIs, that these are the basic models necessary to calculate FCI phenomena; they may need to be supplemented later, as additional effects are discovered, but a code with these basic models should be capable of doing an adequate simulation of FCIs.

Other extensions necessary to IFCI include providing the interfield constitutive relations between the field for molten fuel ("melt") and the water and steam fields, and extending the equation-of-state package for water-steam to allow supercritical pressures and temperatures.

2.2 Code Structure

IFCI was formerly an integral part of the MELPROG code. It is based on MELPROG's FLUIDS module hydrodynamics subroutines. Furthermore, IFCI drivers, input and output routines are derived from MELPROG subroutines. A description of MELPROG's code structure is given in Dosanjh (1989). **Error! Reference source not found.** shows the hierarchy of IFCI subroutines.

2.3 Input and Output

IFCI input routines for problem initialization and restart are derived from those used by MELPROG. An IFCI input deck is similar to that specified by MELPROG's Version 5.2 input description (Heames 1989). However, a number of extraneous parameters have been removed from the input and a number of additional quantities are required by the FCI models. The input deck is described in the input description, Appendix A.

IFCI generates two types of output; printed text and a fluids graphics file. The printed output is iteration information to standard output and text information for the fields, which includes, in addition to standard information (volume fraction, temperature, etc.), a characteristic diameter for melt particles that IFCI calculates for each mesh cell. The graphics file includes standard fluids information, the melt characteristic diameter, and the melt surface area per unit volume for each mesh cell.

The fluid graphics file is usually input to a graphics post-processor, MPOST, which produces output files suitable for use with third-party graphics programs, such as CoVis (CoHort Software 1995) or Tecplot (Amtec Engineering 1993). The file is formatted as an "unpacked comp file," and conforms to the input format for the TRAP postprocessor (Jenks and Martinez 1988) and can also be used with that program, if desired.

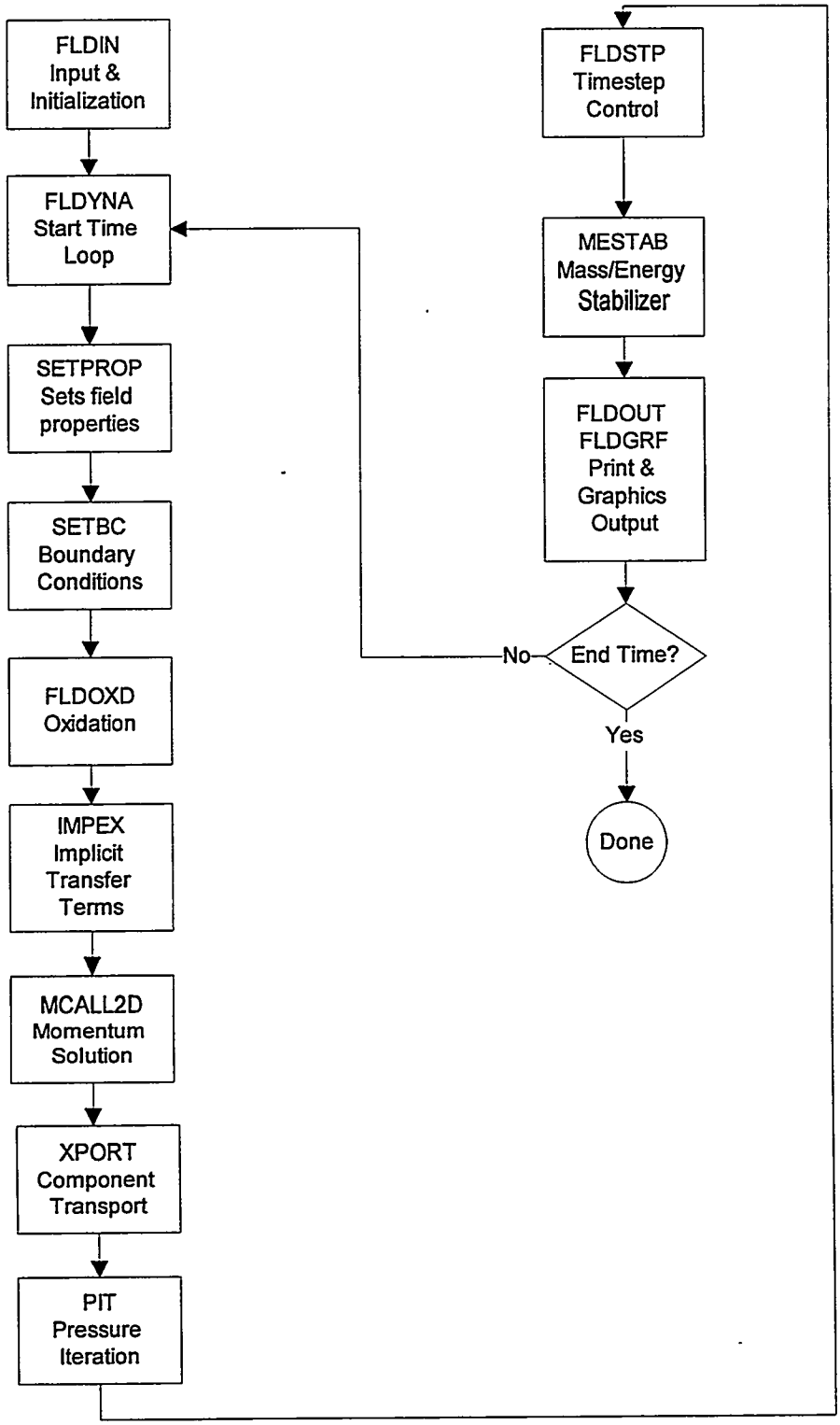

Figure 2-1. Main IFCI routines.

3. BASIS AND ASSUMPTIONS

3.1 Field Equations

The equation set used in IFCI is a three-field, two-dimensional, cylindrical geometry version of a set commonly used in multifield computational hydrodynamics and originally derived from the general field equations of Ishii (Ishii 1975; Kocamustafaogullari 1971). A "field" in the context of multifield hydrodynamics is represented by separate momentum, mass continuity, and energy equations for each type and phase of material in the interaction. These three equations are solved for each "field." Mass, energy, and momentum transfer among fields are represented by coupling terms in the field equations for which constitutive relations must be provided. Also necessary is an equation of state for each field. The field equations, associated constitutive relations, equations of state, and initial and boundary conditions, are solved by a variation of the SETS method developed by Mahaffy (1982).

The field equations used in IFCI (Equations 3.1 through 3.3) are given below for field k and coordinate x:

$$\frac{\partial}{\partial t}(\alpha_k \rho_k)+\nabla\bullet(\alpha_k \rho_k \vec{v}_k)-\Gamma_{jk}-\Gamma_{wk}=0 \tag{3.1}$$

$$\frac{\partial}{\partial t}(\alpha_k \rho_k v_{xk})+\nabla\bullet(\alpha_k \rho_k \vec{v}_k v_{xk})+\alpha_k \frac{\partial P}{\partial x}+\left[\sum_{j=1}^{3} C_{xjk}(v_{xk}-v_{xj})|v_{xk}-v_{xj}|+C_{xwk}\, v_{xk}|v_{xk}|\right]+\alpha_k \rho_k g_x=0 \tag{3.2}$$

$$\frac{\partial}{\partial t}(\alpha_k \rho_k e_k)+\nabla\bullet(\alpha_k \rho_k e_k \vec{v}_k)+P\left(\frac{\partial \alpha_k}{\partial t}+\nabla\bullet\alpha_k \vec{v}_k\right)-\sum_{j=1}^{3}\Gamma_{jk}H_k-\sum_{j=1}^{3}Q_{jk}-Q_{wk}-Q_{sk}=0 \tag{3.3}$$

Finally, a constraint on the sum of the fluid volume fractions is also required:

$$1-\sum_{k=1}^{3}\alpha_k-\alpha_s=0 \tag{3.4}$$

In Equations 3.1 through 3.4, α_k is the volume fraction with respect to the total finite-difference mesh cell volume. There can also be a nonflow volume fraction in the cell, as structures, α_s. The velocity vector $\vec{v}_k$ is composed of axial and radial components v_{zk} and v_{rk}. The third and fourth terms in Equation 3.1 represent mass transfer among the fields and external mass source terms, respectively. The mass transfer between steam and liquid water is treated implicitly in temperature and pressure, while the other mass transfers are explicit sources. In the momentum equation (see Equation 3.2), the fourth term represents momentum transfer among the fields, and the fifth term represents wall friction. The coefficients, C, are evaluated explicitly based on the local flow regime. In the energy equation (see Equation 3.3), the third term is the work term. The fourth term represents energy exchange between the fields due to phase change, with H_k representing the saturation enthalpy. The fifth term represents heat transfer among fields. The sixth term represents external energy sources, and the seventh term is energy transfer to an interface at saturation.

Equations 3.1 through 3.4 constitute a set of thirteen coupled, nonlinear, partial differential equations that, along with material equations of state and constitutive relations for mass, energy, and momentum exchange, form the hydrodynamic equation set of IFCI.

3.2 Closure Equations and Constitutive Relations

The interfield heat transfer terms in Equation 3.3 are given as

$$Q_{jk} = A_{jk} h_{jk} \left(T_k - T_j\right) \tag{3.5}$$

where the interfacial area per unit volume between fields j and k, A_{jk}, and the heat transfer coefficient, h_{jk}, are provided by constitutive relations for each flow regime.

Mass transfer between the water and steam fields is described by a simple bulk boiling model assuming the existence of an interface between the two fields at the saturation temperature:

$$\Gamma_{12} = A_{12} \frac{h_{2\text{sat}} \left(T_2 - T_{\text{sat}}\right) - h_{1\text{sat}} \left(T_1 - T_{\text{sat}}\right)}{H_{lg}} \tag{3.6}$$

Surface boiling at the melt surface is modeled by a subcooled surface boiling model,

$$\Gamma_3 = A_3 \frac{h_{4\text{sat}} \left(T_3 - T_{\text{sat}}\right) - h^c_{2\text{sat}} \left(T_{\text{sat}} - T_2\right)}{H'_{lg}} \tag{3.7}$$

where H'_{lg} is an effective latent heat of vaporization, modified to account for the sensible heat of the vapor. Equation 3.7 is used to describe film boiling at a surface with either saturated or subcooled coolant.

Constitutive relations are provided in IFCI for heat and momentum transfer in the bubbly, slug, and mist flow regimes between water and vapor. Flow regimes for the melt field are derived by treating the water and vapor together as a second phase. The melt is then described, based on the melt volume fraction, as either continuous with entrained vapor-water droplets, or as melt droplets in a continuous vapor-water phase (Young et al. 1998). Provision is also made for the existence of mixture levels; i.e., formation of pools of water or melt.

Heat transfer coefficients (HTCs) between melt and water fields are provided via a boiling curve, which describes nucleate, transition, and film boiling. Only film boiling, the dominant regime for IFCI, is described here. The complete boiling curve is described by Dosanjh (1989). At high vapor volume fractions, a transition is made between film boiling heat transfer to water and convective heat transfer to vapor from the melt.

3.3 Additional IFCI Models

In IFCI, a melt drop is described as an Eulerian melt field interacting with the water and steam fields, which are also Eulerian. The fuel characteristic size may either be smaller than a finite-difference mesh cell (i.e., subgrid size) or extend over more than one cell. In the subgrid case, the fuel melt exists as discrete drops, which IFCI treats with a model for primary breakup. The primary breakup model provides a source term for a continuity (transport) equation for melt volumetric surface area. In the case where the melt extent is larger than the finite-difference grid, surface area generation takes place as the melt geometry distorts due to hydrodynamic motion on the grid. IFCI includes a surface area tracking model/algorithm to treat this case, but the model is currently turned off.

3.4 Finite-Difference Grid

The finite-difference grid in IFCI is shown in Figure 3-1 for reference in setting up IFCI input decks. The main field variables of pressure, volume fraction, and temperature are defined at the cell center, whereas the velocities are defined at the cell edges.

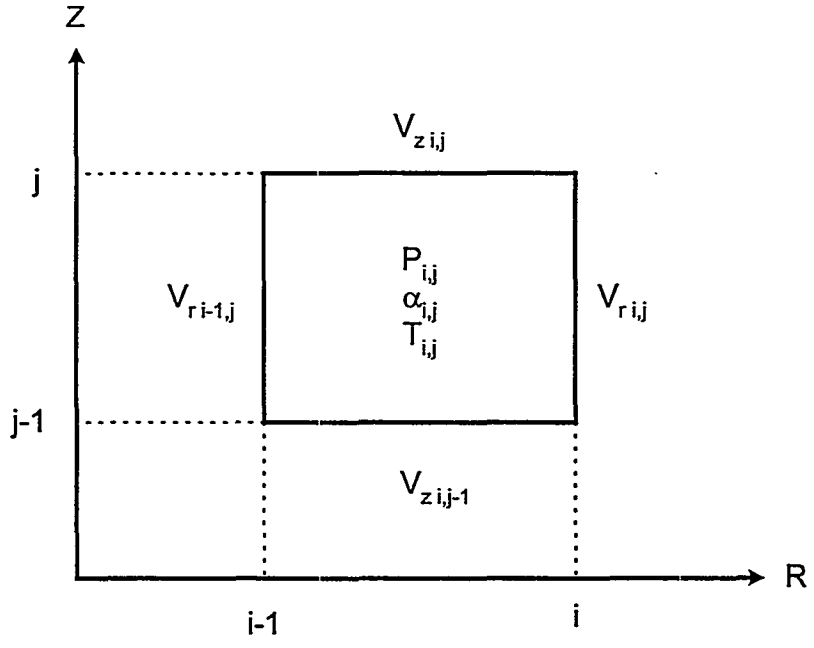

Figure 3-1. IFCI finite-difference cell.

4. QUALITY ASSURANCE

Procedures adopted at SNL to ensure the quality of the IFCI code can be grouped into three general areas:

- Assessment and validation of individual models and correlations. These procedures apply to both the closure relations for the field equations and the models for specific FCI phenomena, such as dynamic fragmentation.
- Assessment and validation of the complete code against FCI experiments.
- Methods used to ensure that the code is soundly developed, so as to be reliably useful to the reactor-safety community. Such methods include those used to ensure configuration control, portability and traceability, providing suitable documentation and use of standardized coding practices.

4.1 Models and Correlations

IFCI solves 2D field equations by the SETS method. The hydrodynamics module used (FLUIDS) is described by Dearing (1985) and by Dosanjh (1989). Schmidt et al. (1990) and Young et al. (1998) give detailed information on the FLUIDS constitutive relations for water and steam. The additional models of specific importance to IFCI that concern FLUIDS field 3, the melt field, are briefly described in Section 3 of this document. Section 3 also provides an extensive set of references. The following subsections provide additional information on the assessment and validation of the models specific to the melt field.

4.1.1 Stripping Model

The primary stripping model has been validated against small-scale drop breakup data, (Pilch 1981; Marshall and Seebold 1985) and medium-scale melt breakup data (Young 1987; Young 1990). The results are reasonable, but the data are not prototypical of FCIs. The sensitivity of IFCI 7.0 results to this model is not certain.

4.1.2 Flow Regimes

The melt-water-steam flow regime descriptions used by IFCI are theoretically derived, but can be compared with available three-field experimental data. Most of these data describe either non-boiling conditions or the behavior of small drops with phase change in an immiscible fluid (Mori 1978). Experimental difficulties have so far precluded observation of actual melt-water-steam flow regimes.

4.1.3 Film Boiling Model

IFCI's film boiling model has been verified for the case of single hot drops surrounded by water (Dhir and Purohit 1977). An unpublished comparison has been done by M. F. Young at SNL against one- and two-dimensional tests performed at Brookhaven National Laboratory in order to verify that steam production is also correct for large ensembles of drops.

4.2 Comparison of Code Results with Experimental Data

Satisfactory validation of IFCI results against the Sandia FITS experiments has been described by Young (1987, 1990) and Dosanjh (1989). An additional validation effort has been carried out by M. F. Young at SNL using data from the Sandia EJET experiments (Marshall and Beck 1987). The EJET series consisted of five experiments in which molten iron/alumina in a jet configuration fell into water chambers. Jet diameters ranged from 3.8 cm to 16.3 cm. Davis (Davis 1993) discusses IFCI 6.0 results for the FITS-D pouring mode experiment, FARO scoping test (Joint Research Center 1992), and explosive FCI data from the IET-8 experiments (Allen et al. 1993) performed at Sandia. Reed (Reed et al. 1995) has performed extensive comparisons of IFCI calculations with MIXA-6, MAGICO, and KROTOS experimental results.

4.3 Model Limitations

IFCI 7.0 is a stand-alone code, designed to model full-scale FCI accident scenarios. It is intended to model thermal FCIs in as mechanistic a manner as possible. Model and integrated code validation has not been performed for all possible situations. Important validation gaps include steam explosions in the suppression pool and reflooding of a degraded core.

Several known limitations exist at this time. The flow regime map requires that the two-dimensional finite-difference nodalization be on a sufficiently large scale that the flow regime described is subgrid scale. Mesh cells that are too small (on the order of 1 cm for the present flow regime maps) can result in code execution failures or incorrect results. Shortcomings are also present as a result of model limitations. These include the parametric models currently available for the triggering phenomenon and detonation.

4.4 Coding Methods

IFCI is written in standard, portable Fortran 77. No special system calls are used except for the date and time calls, which tend to be machine-specific. Library calls are made to SLATEC linear-system solution routines, Fortran versions of which are readily available.

The stand-alone version of IFCI, IFCI 7.0, has been developed for use on multiple computer platforms, and has been documented to exist as baseline software. Additional changes will be documented by SNL memoranda.

IFCI subroutines (i.e., the melt fragmentation, surface tracking, and area transport routines) have a standard subroutine header, consisting of a set of Fortran comments in a standard format based on that in Sandia Software Guidelines, Volume 3, Standards, Practices, and Conventions (1986). This standard header contains the routine's purpose, routines called and called from, and revision history, providing additional traceability.

5. REFERENCES

Abolfadl, M. A. and T. G. Theofanous, 1987, "An Assessment of Steam-Explosion-Induced Containment Failure. Part II: Premixing Limits," *Nucl. Sci. Eng.* **97**, 282-295.

Allen, M. D., T. K. Blanchat, M. Pilch, and R. T. Nichols, 1993, Experiments to Investigate the Effects of Fuel/Coolant Interactions on Direct Containment Heating, The IET-8A and IET-8B Experiments, SAND92-2849, Sandia National Laboratories, Albuquerque, NM.

Amtec Engineering, 1993, *Tecplot Version 6 User's Manual*, Bellavue, WA.

Bankoff, S. G. and A. Hadid, 1984, "The Application of a User-Friendly Code to Nuclear Thermalhydraulic Reactor Safety Problems," in *Proc. Int. Nuclear Power Plant Thermal Hydraulics and Operations Topl. Mtg.*, American Nuclear Society.

Bromley, L. A., N. R. LeRoy, and J. A. Robbers, 1953, "Heat Transfer in Forced Convection Film Boiling," *Ind. Eng. Chem.* **45**, 2639-2646.

Carachalios, C. et al., 1983, "A Transient Two-Phase Model to Describe Thermal Detonations Based on Hydrodynamic Fragmentation," in *Proc. Intl. Mtg. on LWR Severe Accident Evaluation.*

Chu, C. C. and M. L. Corradini, 1989, "One-Dimensional Transient Fluid Model for Fuel/Coolant Interaction Analysis," *Nucl. Sci. Eng.* **101**, 48-71.

CoHort Software 1995, *CoVis*, Minneapolis, MN.

Corradini, M. L., 1981a, Analysis and Modelling of Steam Explosion Experiments, SAND80-2131, NUREG/CR-2072, Sandia National Laboratories, Albuquerque, NM.

Corradini, M. L., 1981b, "Phenomenological Modeling of the Triggering Phase of Small-Scale Steam Explosion Experiments," *Nucl. Sci. Eng.* **78**, 154-170.

Davis, F. J., 1993, "IFCI 6.0 Operational Assessment," letter report to USNRC.

Dearing, J. F., 1985, "A Four-Field Model of PWR Degraded Cores," paper presented at Third International Topical Meeting on Reactor Thermal-Hydraulics.

Dhir, V. K. and G. P. Purohit, 1977, "Subcooled Film- Boiling Heat Transfer from Spheres," paper presented at AICHE-ASME Heat Transfer Conf.

Dosanjh, S. S., 1989, ed., MELPROG-PWR/MOD1: A Two-Dimensional, Mechanistic Core for Analysis of Reactor Code Melt Progression and Vessel Attack Under Severe Accident Conditions, SAND88-1824, NUREG/CR-5193, Sandia National Laboratories, Albuquerque, NM.

Fletcher, D. F. and A. Thyagaraja, 1989, "Multiphase Detonation Modelling using the CULDESAC Code," paper presented at 12th Intl. Colloquium on the Dynamics of Explosions and Reactive Systems.

References

Greene, G. A., T. Ginsberg, N. K. Tutu, 1985, "BNL Severe Accident Sequence Experiments and Analysis Program," in *Proc. Twelfth Water Reactor Safety Research Information Mtg.*, NUREG/CP-0058, **3**.

Heames, T. J., 1989, MELPROG PWR/MOD1 User's Manual, SAND90-0597, Sandia National Laboratories, Albuquerque, NM.

Ishii, M., 1975, *Thermo-Fluid Dynamic Theory of Two-Phase Flow*.

Jenks, R. P. and V. Martinez, 1988, TRAC Support Software, NUREG/CR-5071, Los Alamos National Laboratory, Los Alamos, NM.

Joint Research Center, 1992, FARO LWR Programme : Scoping Test Data Report, Technical Note No. I.92.135, Institute for Safety Technology, Ispra, Italy.

Kelly, J. E., 1985, "MELPROG: An Integrated Model for In-Vessel Melt Progression Analysis," paper presented at Thirteenth Water Reactor Safety Research Information Meeting.

Kim, B., 1985, "Heat Transfer and Fluid Flow Aspects of Small-Scale Single Droplet Fuel-Coolant Interactions," Ph. D. dissertation, University of Wisconsin, Madison, WI.

Kim, B. and M. L. Corradini, 1988, "Modeling of Small- Scale Single Droplet Fuel/Coolant Interactions," *Nucl. Sci. Eng.* **98**, 16-28.

Kocamustafaogullari, G., 1971, "Thermo-Fluid Dynamics of Separated Two-Phase Flow," Ph. D. dissertation, Georgia Inst. of Technology, Atlanta, GA.

Los Alamos Safety Code Development Group, 1986, TRAC- PF1/MOD1: An Advanced Best-Estimate Computer Program for Pressurized Water Reactor Thermal-Hydraulic Analysis, LA-10157-MS NUREG/CR- 3858, Los Alamos National Laboratory, Los Alamos, NM.

Mahaffy, J. H., 1982, "A Stability-Enhancing Two-Step Method for Fluid Flow Calculations," *J. Comp. Phys.* **46**, p. 329.

Marshall, Jr., B. W., 1988, "Recent Fuel-Coolant Interaction Experiments Conducted in the FITS Vessel," paper presented at 25th ASME/AIChE National Heat Transfer Conference.

Marshall, Jr., B. W. and D. F. Beck, 1987, The Coarse Mixing of Boiling and Isothermal Jets, SAND87-2455C, Sandia National Laboratories, Albuquerque, NM.

Marshall, Jr., B. W and O. P. Seebold, 1985, Reactor Safety Research Semiannual Report January-June 1985, Vol. 33, SAND85-1606, pp. 67-71, Sandia National Laboratories, Albuquerque, NM.

Medhekar, S. et al., 1988, "Triggering and Propagation of Steam Explosions," presented at 25th ASME-AIChE Heat Transfer Conference.

Mitchell, D. E. et al., 1981, Intermediate Scale Steam Explosion Phenomena: Experiments and Analysis, SAND81- 0124, NUREG/CR-2145, Sandia National Laboratories, Albuquerque, NM.

Mori, Y. H., 1978, "Configurations of Gas-Liquid Two-Phase Bubbles in Immiscible Liquid Media," *Int. J. Multiphase Flow*, **4**.

Pilch, M., 1981, "Acceleration Induced Fragmentation of Liquid Drops," Ph. D. dissertation, University of Virginia, Charlottesville, VA.

Reed, A. W., M. F. Young, and R. C. Schmidt, 1995, "Results of the IFCI 6.0 Assessment: Calculations of MAGICO-701, MIXA-6, and KROTOS-26 Experiments," letter report to USNRC.

Rightley, M. J., D. F. Beck, and M. Berman, 1991, NPR/FCI EXO-FITS Experiment Series Report, SAND91-1544, Sandia National Laboratories, Albuquerque, NM.

Roache, P. J., 1972, *Computational Fluid Dynamics*, Hermosa Publishers, Albuquerque, NM.

Sandia Software Guidelines, Vol. 3, Standards, Practices, and Conventions, 1986, SAND85-2346, Sandia National Laboratories, Albuquerque, NM.

Schmidt, R. C. et al., 1990, MELPROG PWR/MOD1 Models and Correlations, SAND89-3123, NUREG/CR-5569, Sandia National Laboratories, Albuquerque, NM.

Stevenson, M. G., 1980, Report of the Zion/Indian Point Study, LA-8306-MS, NUREG/CR-1411, Los Alamos National Laboratory, Los Alamos, NM.

Swenson, D. V. and M. L. Corradini, 1981, Monte Carlo Analysis of LWR Steam Explosions, SAND81-1092, NUREG/CR- 2307, Sandia National Laboratories, Albuquerque, NM.

Thyagaraja, A. and D. F. Fletcher, 1986, "Buoyancy-Driven, Transient, Two-Dimensional Thermo-Hydrodynamics of a Melt- Water-Steam Mixture," CLM-P790, UKAEA, Culham Laboratory, Abingdon, UK.

Young, M. F., 1982, "The TEXAS Code for Fuel-Coolant Interaction Analysis," in *Proc. of the LMFBR Safety Topical Meeting, Lyon*.

Young, M. F., 1987, IFCI: An Integrated Code for Calculation of All Phases of Fuel-Coolant Interactions, SAND87-1048, NUREG/CR- 5084, Sandia National Laboratories, Albuquerque, NM.

Young, M. F., 1990, Application of the IFCI Integrated Fuel-Coolant Interaction Code to a FITS-Type Pouring Mode Experiment, in *Dynamics of Detonations and Explosions : Explosion Phenomena*, AIAA, Vol. 134.

Young, M. F., A. W. Reed, and R. C. Schmidt, 1998, IFCI 7.0 Models and Correlations, SAND98-xxxx, Sandia National Laboratories, Albuquerque, NM, to be published.

APPENDIX A : INPUT DESCRIPTION

IFCI Version 7.0

INTRODUCTION

IFCI is derived from the FLUIDS module of the MELPROG/MOD1 severe accident analysis code. As such, the input format is basically the same as that for MELPROG FLUIDS with some extensions for the FCI models in IFCI. Only a few of the input variables have been removed from the MELPROG version of IFCI prior to completion of code assessment. However, a number of calculations are no longer performed when using the stand-alone version of the code.

INPUT DESCRIPTION

IFCI can be run in two modes - an initialization mode or a restart mode. In both modes the necessary input will be read from unit 95, but this file will be substantially smaller during the restart mode because most of the information will be obtained from the restart file (written to unit 98, and read in as unit 93). A skeleton restart file is written to unit 94 during initialization, which can be used as the basis for the restart input file. In the following sections, the initialization input file and the restart input file are described.

GENERAL ORGANIZATION

An IFCI input deck is organized by module and contains the data necessary for problem control as well as fluids, materials, geometry, and initial and boundary conditions. These data are contained on unit 95 and must be in a specified order.

The problem control data input consists of general parameters such as titles, restart and dump information, beginning and ending time, maximum time step, and convergence criteria. These data must always be present on unit 95. The module input consists of the information necessary to specify and control the problem within each module.

FREE FORMAT INPUT STRUCTURE

The data are read into the code using a free format input processor, FUNRD. With this processor, the order in which numbers are read is determined by the code and therefore a card out of order will cause an error. This input processor does not allow for default values, i.e., all required inputs must be entered. Values in the input description that are offset with parentheses are typical values. The typical values may be used in the absence of additional information.

DATA. Data are acceptable as integer, fixed field, or scientific notation. In the latter case, "e" is used to indicate the exponent field. All of the following values will be interpreted equivalently (100 100.0 1.0e2 1.0e+2).

SEPARATORS. Data is delimited by a comma (,) or a space ( ) or the end of the record (column 80).

REPETITION. Repetition of values may be done with the form "n*v", where n is the number of times the value v is to be read. Repetition of groups of values is done with the form "n*(m1*v1, m2*v2, ...), where n is the number of times the group within the parentheses is repeated. The total number of values that can be read on one line is 40; therefore something like "60*0.05" must be broken up into "40*0.05" on one line and "20*0.05" on the following line. Note: there cannot be any separation between the number of values, n, and the asterisk, *, as this will cause the input data to be incorrectly interpreted as successive values.

CONTINUATIONS. Successive values are assumed to be either on the same card or on the next noncomment card; therefore the user may use 1 card to input 5 values or as many as 5 cards.

EXCESS DATA. Additional data on cards are ignored. In the detailed input description that follows, each read statement has been given a number. The user cannot connect read statements; for example, the second read is the restart flag, IRESTRT. Any additional numbers on the card will be flagged by the code as a possible error and ignored.

COMMENT CARDS. A $ in column 1 identifies the card as a comment card. The card will only be printed as read. There is no limit to the number or location of these cards.

UNITS. Systeme International (S.I.) units are used for all IFCI input, as shown in Table A.1.

TABLE DATA. IFCI inputs table data in (x,y) pairs, for example (time, power level) or (time, exit pressure). The code linearly interpolates between points in the table, uses a constant value beyond table limits, and requires a minimum of two table pairs. It should be noted that no warnings are printed for values beyond table limits.

ARRAY DATA. IFCI inputs array data, for example the cell by cell additive friction factors, according to standard FORTRAN rules. This means that the friction factors are input as consecutive axial nodes, from bottom to top, for each radial ring, starting from the innermost ring.

Table A.1. S.I. units used for IFCI

Quantity	S.I. Unit	Quantity	S.I. Unit
Length	m	Density	kg/m^3
Mass	kg	Time	s
Volume	m^3	Power	W
Temperature	K	Pressure	Pa
Velocity	m/s	Viscosity	Pa-s
Surface Tension	kg/s^2	Torque	N-m
Specific Heat	J/kg-K	Thermal Conductivity	W/m-K
Heat Transfer Coefficient	W/m^2-K	Volumetric Heat Source	W/m^3

PROBLEM INITIALIZATION (unit 95)

In the following detailed IFCI input specifications, each READ statement has been given a number, therefore READ statement number 3 is expecting values for DMPINT, GFINT, and EDITN. These values are placed on separate lines or on the same line. After enough lines have been read to yield 3 input values, IFCI will proceed to read statement 4 input beginning with the next line. Any additional information remaining on the current line will be ignored.

GENERAL INPUT

1. ITITLE (20A4)

A. ITITLE = Problem title (up to 80 characters).

2. IRESTRT

A. IRESTRT = The restart switch, set to 0 for initialization.

3. DMPINT, GFINT, EDINT

A. DMPINT = Restart dump interval (s) (unit 98; this file contains the information necessary to restart the code at the end of this interval).

B. GFINT = Graphics dump interval (s) (unit 92; this file contains graphics information.

C. EDINT = Full edit interval (s) (unit 96; this file contains the printed output).

4. PRNTTO

A. PRNTTO = Problem time or step number at which an additional full edit is desired. The logic within the code is such that an input value of 12 would yield a full print at both the 12^{th} step and at 12 seconds. Typically this input is set to a large value or used to examine the calculation at a known time, for example, failure in an experiment.

5. IPRTF, IPRTR, IPRTD

A. IPRTF = FLUIDS module full print flag (0=off, 1=field data, 2=transfer. function data, 3=fluid property data).

B. IPRTR = RADIATION module full print flag (0=off, 1=on).

C. IPRTD = DEBRIS module full print flag (0=off, 1=on).

NOTE: The values chosen for these flags only control the amount of output sent to unit 96. If verifying the input, set these flags to their maximum value; if the code is experiencing problems set IPRTF=2.

6. KMAX, NRING

A. KMAX = Number of axial nodes.

B. NRING = Number of radial rings.

NOTE: The values chosen for KMAX and NRING determine to a large part the total computational time the problem will take.

NOTE: The total number of cells allowed, KMAX*NRING, is controlled by the length of two container arrays within the code, X and XLCM. After the input has been read, the code will determine the total length for these arrays and whether the user has exceeded the

compiled limits. At this time, IFCI does not have a dynamic allocation system capable of making the correct adjustments to these arrays; hence if the user finds that they have exceeded the current limits, they must change the limits in the space.h and lcm1.h common files and recompile the code.

7. GASCOEF

A. GASCOEF = Maximum fraction of the vapor internal energy that the vapor can receive from all heat sources in one time step. This variable will control the time step in many cases (typical values range from 0.05 when the vapor is hot to 0.25 when it is cold).

8. TIME, ENDTIM, DELTO

A. TIME = The starting time (s).

B. ENDTIM = Problem end time (s).

C. DELTO = The initial time step (s). Typically we initially use a small step and allow the code to control the increases. (0.05).

9. NTIM

A. NTIM = Number of time step pairs in the maximum allowable IFCI time step table (> 1).

10. STEP(l,n), l=1,2 n=1,NTIM

A. STEP = Maximum allowable time step table, NTIM pairs of problem time (seconds) and maximum time step (seconds) Typically, values between 0.25 and 1.0 are used for the maximum time step. If the code has time step control problems associated with the explicit links between modules, the user can lower this value to control the calculation.

FLUID DYNAMICS MODULE INPUT

In this section of the input the user will supply most of the data necessary to describe the problem from the FLUIDS point of view.

Fluids Module Input: Scalar Data

11. DTINC

A. DTINC = Maximum allowable fractional time step increase between steps (typical value is 1.05).

12. DTMIN

A. DTMIN = Minimum time step. If the code requires a step size below this value, the problem terminates (s) (typical value is 1.0e-9).

13. CRFAC

A. CRFAC = Courant multiplication factor. This determines a time step due to the fluid Courant condition (mesh size/velocity) times CRFAC. If too large, fluid temperature oscillations will occur (typical values are 1-10).

14. ITERMIN, ITERMAX

A. ITERMIN = Minimum iterations. The time step may only increase if the number of pressure iterations taken in the FLUIDS module is less than ITERMIN (typical values are 3-5).

B. ITERMAX = Maximum number of pressure iterations that can be taken in the FLUIDS module before failure. If the error has been decreasing during the iteration but is still larger than ERROR1, when ITERMAX is reached, the code will print a warning and accept the calculation. If the error is not decreasing, the time step is reduced by 10% and an explicit calculation is executed (typical values are 10-20).

15. ERROR1

A. ERROR1 = Error criterion 1 for the Newton-Raphson iteration. This is the convergence criterion on the change in relative pressure from iteration to iteration in the FLUIDS calculation. The change in pressure from iteration to iteration may not always force the necessary convergence of the velocities and temperatures, therefore we recommend a tight convergence (typical values are 1.0e-9 - 2.0e-5).

16. EPSA

A. EPSA = Maximum fractional change in fluid volume fraction between time steps (typical values are 0.1-0.5).

17. EPST

A. EPST = Maximum fractional change in fluid temperature between time steps (typical values are 0.01-0.1).

18. CONDCOEF

A. CONDCOEF = Coefficient multiplying the bulk condensation rate (1.0e-4).

19. IOXFLAG, IMWRIN

A. IOXFLAG = Metal-water oxidation model flag, 0 = off, 1 = on.

B. IMWRIN = Metal-water rate law override. This is used to select a metal-water reaction rate law other than the default. It is useful for parametric studies, provided that there is only one metal-oxide pair in the system, as only one reaction rate law can be specified (0).

NOTE: DCOR3 is used for the melt-water interaction models and small values will force a significant evaporation rate to occur.

20. DCOR3

A. DCOR3 = Initial characteristic diameter of the molten material in field 3, liquid melt (m) (typical values are 0.02-0.04).

21. MATID3(l), l=1,8

A. MATID3 = Material identifiers (IDs) to be used for field 3 melt properties. If eight 0's are entered, the default materials 1,17,3,4,5,6,13,14 (UO_2, Ag-In-Cd, Zr, ZrO_2, SS, SSOx, INC, INCOx) are used. A value for the total number of materials being considered, ICMPIN, is determined by finding the first 0 in the data. When entering the material IDs, the user should be aware that the oxidation routines

assume that the base metal will be followed in the pattern by the oxide, for example Zr by ZrO_2. If oxidation is considered in the problem, both the metal and its oxide IDs must be entered, even if only metal is present initially. Materials are mixed to determine an average property in accordance with their masses. All the materials in subroutine MATPRO are available as melt material mixtures and their identifying numbers are:

a) MATID3 = 1, UO_2 (Urania).
b) MATID3 = 2, UO_2-PuO_2 mixture.
c) MATID3 = 3, Zircaloy 4.
d) MATID3 = 4, ZrO_2 (zirconia).
e) MATID3 = 5, stainless steel type 304.
f) MATID3 = 6, steel oxide mixture FeO-Cr_2O_3 (Iron chromate).
g) MATID3 = 7, stainless steel type 316.
h) MATID3 = 11, Medium carbon steel type A.
i) MATID3 = 13, Inconel 718.
j) MATID3 = 15, Inconel 600.
k) MATID3 = 17, Ag-In-Cd control rod material.
l) MATID3 = 19, B_4C control rod material.
m) MATID3 = 20, Aluminum metal
n) MATID3 = 21, Al_2O_3 Aluminum oxide.
o) MATID3 = 22, Stoichiometric Fe-Al_2O_3 Thermite.
p) MATID3 = 24, Fe Iron metal, liquid properties.
q) MATID3 = 25, FeO Iron oxide, Wustite.
r) MATID3 = 26, ZrO_2, 91% pure Zirc oxide ceramic, shroud material.
s) MATID3 = 27, ZrO_2 fiber, 79% porous, steam filled, shroud material.
t) MATID3 = 28, ZrO_2 fiber, 79% porous, water filled, shroud material.
u) MATID3 = 29, ZrO_2 fiber, 79% porous, water-steam filled shroud material.

22. FRAC34(l), l=1,8

A. FRAC34 = Reference mass fractions for field 3. These are the initial mass fractions corresponding to the material IDs entered above (MATID3). The melt equation of state (EOS) uses these reference values to determine mass-weighted properties, such as density or heat capacity.

23. PREF

A. PREF = Reference pressure for field 3. The melt thermodynamic EOS uses this parameter (Pa) (see IFCI Models and Correlations document for the form of the EOS).

24. TREF3

A. TREF3 = Reference temperature for field 3. The liquid melt EOS uses this temperature to determine density (K).

25. ASQ3

A. ASQ3 = Inverse sound speed squared for field 3. The liquid melt thermodynamic EOS uses this parameter (s^2/m^2).

26. IDETFLG, IDETTRG, IDETPRP, IFRAG, QVS

A. IDETFLG = Flag to turn detonation models on or off; 0 = off, 1 = on.

B. IDETTRG = Explicit detonation trigger on or off; 0 = off, 1 = on. This allows the user to explicitly specify a cell (JTRG, ITRG) to be triggered at time TIMFRG according to the detonation parameters given below.

C. IDETPRP = Trigger/detonation model selector. Selects a local-hydrodynamic-condition-based trigger/propagation model:

1. 0 = Off.
2. 1 = Pressure threshold model; detonation is triggered when pressure in a cell exceeds a trigger pressure threshold.
3. 2 = Pressure/pressure rise rate threshold model; detonation triggers when pressure and pressure rise rate both exceed threshold levels.

D. IFRAG = Flag to turn fragmentation models on or off; 0 = off, 1 = on.

E. QVS = Artificial viscosity coefficient. This is necessary for shock problems where the numerical diffusion in the differencing scheme may not provide sufficient dispersion. A good value for shocks is around 100.0 (0.0).

THE FOLLOWING LINE IS INCLUDED IF IDETTRG = 1:

27. *for IDETTRG = 1:*
JTRG, ITRG, TIMTRG

A. JTRG = Axial level number for trigger cell.

B. ITRG = Radial ring number for trigger cell.

C. TIMTRG = Time at which to trigger (s).

THE FOLLOWING LINE IS INCLUDED IF IDETPRP > 0:

28. *for IDETPRP = 1:*
PTRG

A. PTRG = Pressure threshold (Pa).

29. *for IDETPRP = 2:*
PTRG, PTRGRAT:

A. PTRG = Pressure threshold (Pa).

B. PTRGRAT = Pressure rise rate threshold (Pa/s).

30. DFRAG, TAUFRAG, IHTDET, HTDET

A. DFRAG = Fine fragment diameter (m).

B. TAUFRAG = Fine fragmentation time (s).

C. IHTDET = Fine fragment heat transfer flag; 0 = use standard correlations, 1 = use input parameter HTDET for heat transfer to fine fragments.

D. HTDET = Fine fragment heat transfer coefficient (W/m^2).

31. ITPTS, IIOUT

A. ITPTS = Number of steps between short FLUIDS prints. (1 line will be printed to standard output and to unit 96).

B. IIOUT = For your information print control; a user-determined value will be edited on short FLUIDS print. A value of IIOUT =:

1. 0 =Consecutive edit of all of the values below (this is the recommended input).
2. 1 =Values of the FLUIDS knobs. A five-digit number consisting of 0's and 1's,

with a 0 indicating that a fluid field is off and a 1 that it is on. The fields are steam, water, solid corium, liquid corium, and hydrogen (10001 = all-vapor mixture of steam and hydrogen).

3. 2 =Total hydrogen generation rate (kg/s).
4. 3 =Maximum cladding temperature (K).
5. 4 =Maximum heat transfer coefficient between a rod and vapor (W/m^2-K).
6. 5 =Maximum power generation due to oxidation (W/m^3).
7. 6 =Maximum power transferred to either the vapor or the water fields (W/m^3).
8. 7 =Maximum net heat flow between water and vapor (W/m^3).
9. 8 =Maximum pressure in vessel (Pa).
10. 9 =Liquid temperature exiting the vessel (K).
11. 10 =Vapor temperature exiting the vessel (K).
12. 11 =Total steam generation rate (kg/s).
13. 12 =Volume of liquid water in vessel (m^3).
14. 13 =Total mass divergence, a measure of the conservation of mass within the FLUIDS calculation (kg).

Fluids Module Input: Array Data

NOTE: The additive friction factors for each field (vapor, liquid, liquid corium) have the following uses:

(1) To allow or prevent flow between adjacent cells (input 0.0 and > 1.0e20 respectively). This enables the user to model internal structures, which are not explicitly modeled, but may restrict axial, or radial, flow.

(2) To throttle the flow to get the correct cell to cell flow velocities at steady conditions. The FLUIDS module uses cell edge velocities and cell-centered pressures; the additive friction factor is pressure drop / (avg cell height/hydraulic diam) / kinetic energy, where k.e. = [0.5*rho*vel*abs(vel)]. Typical values for velocities and pressure drops come from either other codes or experimental measurements.

32. NADR

A.	NADR	=	Number of regions for additive friction factors. Each region will be bounded by ILFT, JBOT, IRIGHT, and JTOP.

NOTE: The following boundaries and axial/radial friction factors are input as a group (lines 33-39) NADR times, one group for each region.

33. ILFT, JBOT, IRIGHT, JTOP

A.	ILFT	=	Ring number of first cell on left boundary of region.
B.	JBOT	=	Axial node number of lowest cell in region.
C.	IRIGHT	=	Ring number of last cell on right boundary of region.
D.	JTOP	=	Axial node number of highest cell in region.

NOTE: The radial direction is described by rings, or cells, e.g., RING 1, is bounded by the first radial node (at 0.0) on the interior, and the second radial node on the exterior or right-hand side. The axial direction is described by the axial nodes.

34. ADKZ(j,i), j=JBOT,JTOP i=ILFT,IRIGHT
A. ADKZ = Additive axial friction factor applied at top of axial node J in ring I for field 1, vapor.
35. ADKZ(j,i), j=JBOT,JTOP i=ILFT,IRIGHT
A. ADKZ = Additive axial friction factor applied at top of axial node J in ring I for field 2, water.
36. ADKZ(j,i), j=JBOT,JTOP i=ILFT,IRIGHT
A. ADKZ = Additive axial friction factor applied at top of axial node J in ring I for field 3, liquid corium.
37. ADKR(j,i), j=JBOT,JTOP i=ILFT,IRIGHT
A. ADKR = Additive radial friction factor applied at right-hand face of axial node J in ring I for field 1, vapor.
38. ADKR(j,i), j=JBOT,JTOP i=ILFT,IRIGHT
A. ADKR = Additive radial friction factor applied at right-hand face of axial node J in ring I for field 2, water.
39. ADKR(j,i), j=JBOT,JTOP i=ILFT,IRIGHT
A. ADKR = Additive radial friction factor applied at right-hand face of axial node J in ring I for field 3, liquid corium.

Fluids Module Input: Boundary Conditions

NOTE: The code assumes that no fluid field can either enter or exit the problem domain (the outer ring and the bottom and top axial nodes). To allow inflow and outflow to the problem domain, the following input is needed. The current version of the code only allows inflow and outflow at the outer boundaries.

40. NINBC
A. NINBC = Number of cell locations used for inflow boundary conditions (NINBC must be <6).

NOTE: The following inflow boundary condition parameters are repeated as a group (lines 41-53) NINBC times, one group for each inflow location.

41. INN
A. INN = For either a top or bottom inflow boundary condition, INN is the radial ring number whose lower interface coincides with the inflow boundary, 1 <= INN <= NRING. For an inflow boundary on the right face, INN = NRING+1.
42. JIN
A. JIN = For a right boundary condition, JIN is the axial node number whose outer interface coincides with the inflow boundary, 1 <= JIN <= KMAX. For a top boundary condition, this will be KMAX+1. For a

bottom boundary condition, JIN = 0.

43. ARIN

A. ARIN = Flow area at the inflow boundary (m^2). Typically a mass flow is known and this input is used to relate the known flow to the inlet tables below.

44. NPRIN

A. NPRIN = Number of entries in inflow pressure condition tables (< 100).

45. NVIN

A. NVIN = Number of entries in inflow boundary condition velocity tables (< 100).

46. NTIN

A. NTIN = Number of entries in inflow boundary condition temperature tables (< 100).

47. NAIN

A. NAIN = Number of entries in inflow boundary condition volume fraction tables (< 100).

NOTE: The inflow pressure tables are only used to determine the physical properties of the incoming fluid and not the pressure in the problem.

48. PRNTAB(l,n), l=1,2 n=1,NPRIN

A. PRNTAB = Inflow total pressure table, NPRIN pairs of time (s) and pressure (Pa).

49. PH2TAB(l,n), l=1,2 n=1,NPRIN

A. PH2TAB = Inflow hydrogen partial pressure table, NPRIN pairs of time (s) and pressure (Pa). Must be less than the values in PRNTAB except in the case of a pure noncondensable, in which case PH2TAB = PRNTAB.

NOTE: The following velocity, temperature, and volume fraction inflow tables (lines 50-52) are input as a group for each of the 3 inflow fields. The mass fractions (line 53) are also input if field 3 is in the inflow.

50. VINTAB(l,n), l=1,2 n=1,NVIN

A. VINTAB = Inflow boundary condition velocity table for a field, NVIN pairs of time (s) and velocity (m/s). Positive velocity direction is from the bottom to the top and from the centerline to the radial boundary. This means that an inflow on a radial boundary has negative values for velocity.

51. TINTAB(l,n), l=1,2 n=1,NTIN

A. TINTAB = Inflow boundary condition temperature table for a field, NTIN pairs of time (s) and temperature (K).

52. AINTAB(l,n), l=1,2 n=1,NAIN

A. AINTAB = Inflow boundary condition volume fraction table for a field, NAIN pairs of time (s) and fraction. The sum of the volume fractions for all fields should be unity.

53. FRC34(m), m=1,8

A. FRC34 = Mass fractions of the inflow melt. Input mass fraction is input for field 3 if the volume fraction for field 3 indicates its presence. If field 3 will not be in the inflow, this input is not read. Mass fractions are between 0.0 and 1.0.

****Begin outflow pressure boundary condition section; this pressure is used to determine the pressure within the problem.

54. NPBC

A. NPBC = Number of locations for outlet pressure boundary conditions (<6)

Note: The following outflow boundary condition parameters, are repeated as a group (lines 55-60) NPBC times, one group for each outflow location.

55. MPBC

A. MPBC = Boundary condition location flag (outer radial = 1, top axial =2).

56. MOUT

A. MOUT = Axial node for radial outflow pressure boundary condition, if MPBC=1. Radial ring for axial outflow pressure boundary condition, if MPBC=2. This is always on the outside of the mesh, so if MPBC=1 then 1 <= MOUT <= KMAX, and if MPBC=2 then 1 <= MOUT <= NRING. Note that having an inflow and an outflow on the right face of the same cell will cause unrealistic answers.

57. AROUT

A. AROUT = Outflow area (m^2).

58. HDOUT

A. HDOUT = Outflow hydraulic diameter (m).

59. NPROUT

A. NPROUT = Number of entries in outflow pressure boundary condition table (< 100).

60. PROTAB(l,n), l=1,2 n=1,NPROUT

A. PROTAB = Outflow pressure boundary condition table, NPROUT pairs of time (s) and pressure (Pa).

Fluids Module Input: Initial Conditions

NOTE: The following input initializes the problem domain in terms of pressure, temperature, velocities, volume fraction, and mass fraction. The values are input as constants over a region; variations in pressure across region boundaries are difficult for the code unless the additive friction at the boundary is sufficient.

61. NRGIN

A. NRGIN = Number of regions for initial conditions, must initialize problem domain.

NOTE: The following region boundaries and initial conditions are input as a group (lines 62-69) NRGIN times, one group for each region.

62. ILFT, JBOT, IRIGHT, JTOP

A. ILFT = Ring number of first cell on left boundary of region.

B. JBOT = Axial node number of lowest cell in region.

C. IRIGHT = Ring number of last cell on right boundary of region.

D. JTOP = Axial node number of highest cell in region.

63. PIN, PINH2

A. PIN = Total pressure in the region (spatially uniform) (Pa).

B. PINH2 = Hydrogen partial pressure in the region (Pa).

64. ALIN(k), k=1,3

A. ALIN = Initial fluid volume fraction for field K. The sum of the three fluid volume fractions should be 1.0.

65. FRAC3(m), m=1,8

A. FRAC3 = Initial eutectic mass fractions in the region for field 3, input only if ALIN(3) > 0. The input pattern is the same as used in the inflow boundary conditions for field 3. The default pattern is UO_2, AIC, Zr, ZrO_2, SS, SSOx, INC, INCOx. Note that mass fractions are between 0.0 and 1.0.

66. TIN(k), k=1,3

A. TIN = Initial temperature in the region for field k (K).

67. VIN(k), k=1,3

A. VIN = Initial axial velocity (spatially uniform) in the region for field k (m/s).

68. VRIN(k), k=1,3

A. VRIN = Initial radial velocity (spatially uniform) in the region for field k (m/s). This value is typically much smaller than VIN.

69. AL10

A. AL10 = Low-volume fraction limit for all fields. If the volume fraction of a fluid field is calculated to be below this value, the FLUIDS calculation (mass, energy, and momentum) for that field is turned off for the next time step. (1.0e-8 - 1.0e-5, function of whether the case has a low (0.1MPa) or high (10.0MPa) pressure, respectively).

Fluid Module Input: Geometry Data

70. DZ(j), j=1,KMAX

A. DZ = Length of each axial node (m). Avoid order-of-magnitude changes from node to node. Attempt to place the midpoint of nodes near known thermocouple junctions. If a critical phenomenon is anticipated to happen at a particular location, add an extra cell to help define it better.

71. RA(i), i=1,NRING+1

A. RA = Radial position of rings (m). Note that there are NRING+1 of these, starting at RA(1)=0 and going to outer edge of problem.

<<INPUT UNUSED BELOW THIS POINT>>

STRUCTURES MODULE INPUT

The STRUCTURES module input was used to describe all structures, and place them on the computational mesh. No longer used, so use defaults suggested below.

Structures Module Input: Scalar Data

72. MAXMOD, STCNVG, SFCNVG, ITCRST, ITMELT

A. MAXMOD = Number of unique structure models to be input. If set = 0, no structure heat transfer or stress analysis calculation and no additional input are required beyond the 5 values indicated on this card.

B. STCNVG = Freezing and melting convergence criterion.

C. SFCNVG = Crust freezing and melting convergence criterion.

D. ITCRST = Maximum iterations on crust.

E. ITMELT = Maximum iterations on structure melting.

Suggested values: 0 0.1 0.1 5 5

RADIATION HEAT TRANSFER MODULE INPUT

The RADIATION module input allows the user to control the radiation heat transfer calculation.

73. NGROUP

A. NGROUP = Number of radiation groups (1)

74. ITRMAX

A. ITRMAX = Max number of iterations (50, for FLUID axial cell heights substantially larger than the radius, 100 or more if they become more comparable in size).

75. RCONV

A. RCONV = Radiation convergence criterion (1.0e-4, if this error is exceeded by an order of magnitude; then ITRMAX should be increased).

76. TBOUND

A. TBOUND = Radiation boundary sink temperature (300 K).

77. EMISS(k), k=1,6

A. EMISS = Emissivity of structure K. The structures are rods, outer wall, inner wall, bottom plate, top plate, and debris. (We typically use a value of 0.3 for the solid structures and 0.8 for the debris bed.)

78. RFAC, ARHOL, ARHOC, ARHOM

A. RFAC = Planck mean absorption coefficient multiplier for steam (1.0). Subprogram FKPM provides the value for the coefficient as a function of pressure and temperature; RFAC allows the user to adjust the level.

B. ARHOL = Liquid absorption coefficient (a typical range is 0.05-0.10).

C. ARHOC = Solid corium absorption coefficient (0.1, assumes an oxidized surface and high temperatures).

D. ARHOM = Liquid corium absorption coefficient (0.1).

DEBRIS MODULE INPUT

The DEBRIS module input allows the user to control the model through the formation, meltdown, and existence of the calculation.

79.	LDBRIS		
A.	LDBRIS	=	DEBRIS module calculation switch (0=off, 1=on) (0).
80.	NZMAX, NBEDM, ICOND		
A.	NZMAX	=	Maximum number of nodes in a bed (40-60).
B.	NBEDM	=	Maximum number of beds (1).
C.	ICOND	=	Effective conductivity model indicator (1).
1.	ICOND	=	1, The Imura-Takegoshi—Vortmeyer model is used.
2.	ICOND	=	2, The Willhite-Kunii-Smith—Luikov model is used.
81.	ALFDBM, PORMAX, DZMIN, DEFF, SO		
A.	ALFDBM	=	Minimum corium fraction in a cell to initiate the DEBRIS module. (0.60)
B.	PORMAX	=	Maximum allowable porosity (void fraction) in a bed (0.55). If a cell in the bed becomes more porous than this value, the code collapses the cell above into it.
C.	DZMIN	=	Minimum DEBRIS module cell mesh size (0.05 m).
D.	DEFF	=	Effective particle diameter in the bed (0.10 m).
E.	SO	=	Specific power (W/kg). This should first be set to the total initial power divided by the total mass of UO_2. The user should then reduce this value by approximately 20% to account for the release of the volatile fission products (0).

PROBLEM RESTARTS

GENERAL ORGANIZATION

Two data files are required to restart an IFCI calculation, unit 93 (restart file) and unit 95 (input file). As IFCI runs, it creates the file, unit 98, which is a binary file containing restart information. Before running a restart, unit 98 must be copied to unit 93. Then, when IFCI is run in restart mode, unit 93 is used as the reference restart data source.

The user input data file for a restart is unit 95 (the same file name as the problem initial input file) and the input required is similar to that required for the initial problem input. Fluid initialization input is not required. In addition, several parameters can take the previously set value, by specifying the restart value as 1.1e37. Either the skeleton restart file on unit 94 can be copied to unit 95, or the original input deck can be copied without those parts and then modified as necessary.

Restart input data are used to describe the current vessel conditions. It is of three types:
(1) data that must be entered--such as titles and problem end times,
(2) data that should be read from the restart file to get its last or original value--such as the time step or mesh size, and
(3) data that may be either entered or read from the restart.

The flag that tells IFCI to obtain the data for a particular entry from the restart file is the input value 1.1e37. The type of data needed for each of the three types of data in the restart input file is indicated in the input instructions as "enter", as "1.1e37", or as "either" respectively.

GENERAL INPUT

1. ITITLE (20A4) (enter).
A. ITITLE = Problem title (up to 80 characters).
2. IRESTRT (enter).
A. IRESTRT = The restart switch
   a. IRESTRT = 1 Read the first restart dump on unit 93; this will correspond to a restart saved at the beginning of step 1.
   b. IRESTRT = N Read the restart corresponding to step N from unit 93.
   c. IRESTRT = -1 Read the final restart dump from unit 93. This is the typical value for this input on restarts.
3. DMPINT, GFINT, EDINT (enter).
A. DMPINT = Restart dump interval (s) (unit 98).
B. GFINT = Graphics dump interval (s) (unit 92).
C. EDINT = Full edit interval (s) (unit 96).
4. PRNTTO (enter)
A. PRNTTO = Problem time or step number at which an additional full edit is desired. The logic within the code is such that an input value of 12 would yield a full print at both the 12^{th} step and at 12s.
5. IPRTF, IPRTR, IPRTD (enter).
A. IPRTF = FLUIDS module full print flag (0=off, 1=field data, 2=transfer

function data, 3=fluid property data).

B. IPRTR = RADIATION module full print flag (0=off, 1=on).

C. IPRTD= DEBRIS module full print flag (0=off, 1=on).

NOTE: The values chosen for these flags only control the amount of output sent to unit 96 (text output). If verifying the input, set these flags to their maximum value; if little is happening, set all flags to 1; if the code is experiencing problems, set IPRTF=2.

6. KMAX, NRING (1.1e37).

A. KMAX = Number of axial mesh nodes.

B. NRING = Number of radial rings.

7. GASCOEF (either).

A. GASCOEF = Maximum fraction of gas internal energy that the gas can receive as a heat source in one time step.

8. TIME, ENDTIM, DELTO (either).

A. TIME = The starting time (s).

B. ENDTIM = Problem end time (s).

C. DELTO = The initial time step (s). Typically this value is input as 1.1e37 to allow the code to control the time step.

9. NTIM (enter).

A. NTIM = Number of time step pairs in maximum allowable time step table (> 1).

10. STEP(l,n), l=1,2 n=1,NTIM (either).

A. STEP = Maximum allowable time step table, NTIM pairs of problem time (seconds) and maximum time step (s). Typically, values between 0.25-1.0 are used for the maximum time step. If the code has time step control problems associated with the explicit links between modules, the user can lower this value to control the calculation.

FLUID DYNAMICS INPUT

Fluids Module Input: Scalar Data

11. DTINC (either).

A. DTINC = Maximum allowable fractional time step increase between steps.

12. DTMIN (either).

A. DTMIN = Minimum time step. Below this value the problem terminates (s).

13. CRFAC (either).

A. CRFAC = Courant multiplication factor.

14. ITERMIN, ITERMAX (enter).

A. ITERMIN = Minimum number of FLUID module pressure iterations.

B. ITERMAX = Maximum number of FLUID module pressure iterations.

15. ERROR1 (either).

A. ERROR1 = This is the convergence criterion on the change in relative pressure from iteration to iteration. Lowering this value to 1.0e-9 can help provide more stable numerical solutions.

16. EPSA (either).

A. EPSA = Maximum fractional change in fluid volume fraction between time steps.

17. EPST (either).

A. EPST = Maximum fractional change in fluid temperature between time steps.

18. CONDCOEF (either)

A. CONDCOEF = Condensation coefficient multiplies the condensation rate (1.0e-4).

19. IOXFLAG, IMWRIN

A. IOXFLAG = Metal-water oxidation model flag; 0 = off, 1 = on.

B. IMWRIN = Metal-water rate law override. This is used to select a metal-water reaction rate law other than the default. It is useful for parametric studies, provided that there is only one metal-oxide pair in the system, as only one reaction rate law can be specified (0).

20. DCOR3 (either).

A. DCOR3 = Particle diameter used in melt field 3 (m).

21. FRAC34(l), l=1,8

A. FRAC34 = Reference mass fractions for field 3. These are the initial mass fractions corresponding to the material id's entered in the initial problem start. The liquid melt equation of state (EOS) uses these reference values to determine mass-weighted properties, such as density or heat capacity.

22. PREF

A. PREF = Reference pressure for field 3. The melt thermodynamic EOS uses this parameter (Pa) (see IFCI Models and Correlations document for the form of the EOS).

23. TREF3

A. TREF3 = Reference temperature for field 3. The melt caloric and thermodynamic EOSs use this parameter (K).

24. ASQ3

A. ASQ3 = Inverse sound speed squared for field 3. The liquid melt thermodynamic EOS uses this parameter. (s^2/m^2).

25. IDETFLG, IDETTRG, IDETPRP, IFRAG, QVS

A. IDETFLG = Flag to turn detonation models on or off; 0 = off, 1 = on.

B. IDETTRG = Explicit detonation trigger on or off; 0 = off, 1 = on. This allows the user to explicitly specify a cell (JTRG, ITRG) to be triggered at time TIMFRG according to the detonation parameters given below.

C. IDETPRP = Trigger/detonation model selector. Selects a local-hydrodynamic-condition-based trigger/propagation model:

   a. 0 = Off.

   b. 1 = Pressure threshold model; detonation is triggered when pressure in a cell exceeds a trigger pressure threshold.

   c. 2 = Pressure/pressure rise rate threshold model; detonation triggers when pressure and pressure rise rate both exceed threshold levels.

D. IFRAG = Flag to turn fragmentation models on or off; 0 = off, 1 = on.

E. QVS = Artificial viscosity coefficient.

THE FOLLOWING LINE IS INCLUDED IF IDETTRG = 1:

26. *for IDETTRG = 1:*
JTRG, ITRG, TIMTRG

A. JTRG = Axial level number for trigger cell.
B. ITRG = Radial ring number for trigger cell.
C. TIMTRG = Time at which to trigger (s).

THE FOLLOWING LINE IS INCLUDED IF IDETPRP > 0:

27. *for IDETPRP = 1:*
PTRG

A. PTRG = Pressure threshold (Pa).

28. *for IDETPRP = 2:*
PTRG, PTRGRAT:

A. PTRG = Pressure threshold (Pa).
B. PTRGRAT = Pressure rise rate threshold (Pa/s).

29. DFRAG, TAUFRAG, IHTDET, HTDET

A. DFRAG = Fine fragment diameter (m).
B. TAUFRAG = Fine fragmentation time (s).
C. IHTDET = Fine fragment heat-transfer flag; 0 = use standard correlations, 1 = use input parameter HTDET for heat-transfer to fine fragments.
D. HTDET = Fine fragment heat transfer coefficient (W/m^2).

30. ITPTS, IIOUT (enter).

A. ITPTS = Number of steps between short FLUID prints (on TTY and unit 96).
B. IIOUT = For your information print control, edited on short FLUIDS print (0). A value of:
   a. 0 =Consecutive edit of all of the values below (this is the recommended input).
   b. 1 =Values of the FLUIDS knobs; a 5-digit number consisting of 0 and 1's, with a 0 indicating that a fluid field is off and a 1 that it is on. The fields are steam, water, solid melt, liquid melt, and hydrogen (10001 = all-vapor mixture of steam and hydrogen).
   c. 2 =Total hydrogen generation rate (kg/s).
   d. 3 =Maximum cladding temperature (K).
   e. 4 =Maximum heat-transfer coefficient between a rod and vapor (W/m^2-K).
   f. 5 =Maximum power generation due to oxidation (W/m^3).
   g. 6 =Maximum power transferred to either the vapor or the water fields (W/m^3).
   h. 7 =Maximum net heat flow between water and vapor (W/m^3).
   i. 8 =Maximum pressure in vessel (Pa).
   j. 9 =Liquid temperature exiting the vessel (K).
   k. 10 =Vapor temperature exiting the vessel (K).
   l. 11 =Total steam generation rate (kg/s).
   m. 12 =Volume of liquid water in vessel (m^3).
   n. 13 =Total mass divergence; a measure of the conservation of mass within the FLUIDS calculation (kg).

Fluids Module Input: Array Data

NOTE: The additive friction factors for each field (vapor, liquid, solid melt, liquid melt) have the following uses:

(1) To allow or prevent flow between adjacent cells (inputs 0.0 and > 1.0e20 respectively). This enables the user to model internal structures, which are not explicitly modeled, but may restrict axial or radial flow.

(2) To throttle the flow to get the correct cell-to-cell flow velocities at steady conditions. The FLUIDS module uses cell edge velocities and cell-centered pressures; the additive friction factor is pressure drop / (avg cell height/hydraulic diam) / kinetic energy, where k.e. = [0.5*rho*vel*abs(vel)]. Typical values for velocities and pressure drops come from either other codes or experimental measurements.

31. NADR

A.	NADR	=	Number of regions for additive friction factors. Each region will be bounded by ILFT, JBOT, IRIGHT, and JTOP (1, best to initialize entire problem domain).

NOTE: The following boundaries and axial/radial friction factors are input as a group NADR times, one group for each region.

32. ILFT, JBOT, IRIGHT, JTOP

A.	ILFT	=	Ring number of first cell on left boundary of region.
B.	JBOT	=	Axial node number of lowest cell in region.
C.	IRIGHT	=	Ring number of last cell on right boundary of region.
D.	JTOP	=	Axial node number of highest cell in region.

NOTE: The radial direction is described by rings or cells, e.g., RING 1 is bounded by the first radial node (at 0.0) on the interior, and the second radial node on the exterior or right-hand side. The axial direction is described by the axial nodes.

33. ADKZ(j,i), j=JBOT,JTOP i=ILFT,IRIGHT

A.	ADKZ	=	Additive axial friction factor applied at top of axial node J in ring I for field 1, vapor.

34. ADKZ(j,i), j=JBOT,JTOP i=ILFT,IRIGHT

A.	ADKZ	=	Additive axial friction factor applied at top of axial node J in ring I for field 2, water.

35. ADKZ(j,i), j=JBOT,JTOP i=ILFT,IRIGHT

A.	ADKZ	=	Additive axial friction factor applied at top of axial node J in ring I for field 3, liquid melt. Melt will pour through most plates.

36. ADKR(j,i), j=JBOT,JTOP i=ILFT,IRIGHT

A.	ADKR	=	Additive radial friction factor applied at right-hand face of axial node J in ring I for field 1, vapor.

37. ADKR(j,i), j=JBOT,JTOP i=ILFT,IRIGHT

A. ADKR = Additive radial friction factor applied at right-hand face of axial node J in ring I for field 2, water.

38. ADKR(j,i), j=JBOT,JTOP i=ILFT,IRIGHT

A. ADKR = Additive radial friction factor applied at right-hand face of axial node J in ring I for field 3, liquid melt.

Fluids Module Input: Boundary Conditions

NOTE: The code assumes that no fluid field can either enter or exit the problem domain (the outer ring and the bottom and top axial nodes). To allow inflow and outflow to the problem domain, the following input is needed. The current version of the code only allows inflow and outflow at the outer boundaries.

39. NINBC

A. NINBC = Number of cell locations used for inflow boundary conditions (<6).

NOTE: The following inflow boundary condition parameters are repeated as a group NINBC times, one group for each inflow location.

40. INN

A. INN = For either a top or bottom inflow boundary condition, INN is the radial ring number whose lower interface coincides with the inflow boundary, 1 <= INN <= NRING. For an inflow boundary on the right face, INN = NRING+1.

41. JIN

A. JIN = For a right boundary condition, JIN is the axial node number whose outer interface coincides with the inflow boundary, 1 <= JIN <= KMAX. For a top boundary condition, this will be KMAX+1. For a bottom boundary condition, JIN = 0.

42. ARIN

A. ARIN = Flow area at the inflow boundary (m^2). Typically a mass flow is known and this input is used to relate the known flow to the inlet tables below.

43. NPRIN

A. NPRIN = Number of entries in inflow pressure condition tables (< 100).

44. NVIN

A. NVIN = Number of entries in inflow boundary condition velocity tables (< 100).

45. NTIN

A. NTIN = Number of entries in inflow boundary condition temperature tables (< 100).

46. NAIN

A. NAIN = Number of entries in inflow boundary condition volume fraction tables (< 100).

NOTE: The inflow pressure tables are only used to determine the physical properties of the incoming

fluid and not the pressure in the problem.

47. PRNTAB(l,n), l=1,2 n=1,NPRIN
A. PRNTAB = Inflow total pressure table, NPRIN pairs of time (s) and pressure (Pa).
48. PH2TAB(l,n), l=1,2 n=1,NPRIN
A. PH2TAB = Inflow hydrogen partial pressure table, NPRIN pairs of time (s) and pressure (Pa). Must be less than the values in PRNTAB except in the case of a pure noncondensable, in which case PH2TAB = PRNTAB.

NOTE: The following velocity, temperature, volume fraction, and mass fraction inflow tables are input as a group for each of the 3 inflow fields.

49. VINTAB(l,n), l=1,2 n=1,NVIN
A. VINTAB = Inflow boundary condition velocity table for a field, NVIN pairs of time (s) and velocity (m/s). Positive velocity direction is from the bottom to the top and from the centerline to the radial boundary. This means that an inflow on a radial boundary has negative values for velocity.
50. TINTAB(l,n), l=1,2 n=1,NTIN
A. TINTAB = Inflow boundary condition temperature table for a field, NTIN pairs of time (s) and temperature (K).
51. AINTAB(l,n), l=1,2 n=1,NAIN
A. AINTAB = Inflow boundary condition volume fraction table for a field, NAIN pairs of time (s) and fraction. The sum of the volume fractions for all fields should be unity.
52. FRC34(m), m=1,ICMPIN
A. FRC34 = Mass fractions of the inflow eutectics. Input mass fraction is input for field 3 if the volume fraction for field 3 indicates its presence. If field 3 will not be in the inflow, this input is <u>not</u> read. The value for ICMPIN and the component pattern is determined from the input to MATID3, card 20.

****Begin outflow pressure boundary condition section; this pressure is used to determine the pressure within the problem.

53. NPBC
A. NPBC = Number of locations for outlet pressure boundary condition's (<6).

Note: The following outflow boundary condition parameters are repeated as a group NPBC times, one group for each outflow location.

54. MPBC
A. MPBC = Boundary condition location flag (outer radial = 1, top axial =2).
55. MOUT

A. MOUT = Axial node for radial outflow pressure boundary condition, if MPBC=1. Radial ring for axial outflow pressure boundary condition, if MPBC=2. This is always on the outside of the mesh, so if MPBC=1 then 1 <= MOUT <= KMAX, and if MPBC=2 then 1 <= MOUT <= NRING. Note that having an inflow and an outflow on the right face of the same cell will cause unrealistic answers.

56. AROUT

A. AROUT = Outflow area (m^2).

57. HDOUT

A. HDOUT = Outflow hydraulic diameter (m).

58. NPROUT

A. NPROUT = Number of entries in outflow pressure boundary condition table (< 100).

59. PROTAB(l,n), l=1,2 n=1,NPROUT

A. PROTAB = Outflow pressure boundary condition table, NPROUT pairs of time (s) and pressure (Pa).

STRUCTURES MODULE INPUT

The STRUCTURES module input is used to describe all structure, and place them on the computational mesh. All structures must have at least one surface on a FLUIDS cell interface; this is mandatory. The code allows the user to place structures in their actual locations, thus allowing the code to make reasonable radiation and heat-transfer calculations. This module is seldom used.

Structures Module Input: Scalar Data

60. MAXMOD, STCNVG, SFCNVG, ITCRST, ITMELT

A. MAXMOD = Number of unique structure models to be input. If set = 0, no structure heat transfer or stress analysis calculation and no additional input are required beyond the 5 values indicated on this card.

B. STCNVG = Freezing and melting convergence criterion.

C. SFCNVG = Crust freezing and melting convergence criterion.

D. ITCRST = Maximum iterations on crust.

E. ITMELT = Maximum iterations on structure melting.

RADIATION HEAT TRANSFER MODULE INPUT

The radiation module input allows the user to control the radiation heat-transfer calculation.

61. NGROUP

A. NGROUP = Number of radiation groups (1)

62. ITRMAX

A. ITRMAX = Max number of iterations (50, for FLUID axial cell heights substantially larger than the radius, 100 or more if they become more comparable in size).

63. RCONV

A. RCONV = Radiation convergence criterion (1.0e-4; if this error is exceeded by an order of magnitude, then ITRMAX should be increased).

64. TBOUND

A. TBOUND = Radiation boundary sink temperature (K).

65. EMISS(k), k=1,6

A. EMISS = Emissivity of structure K. The structures are rods, outer wall, inner wall, bottom plate, top plate, and debris. (We typically use a value of 0.3 for the solid structures and 0.8 for the debris bed).

66. RFAC, ARHOL, ARHOC, ARHOM

A. RFAC = Planck mean absorption coefficient multiplier for steam (1.0). Subprogram FKPM provides the value for the coefficient as a function of pressure and temperature. RFAC allows the user to adjust the level.

B. ARHOL = Liquid absorption coefficient (a typical range is 0.05-0.10).

C. ARHOC = Solid melt absorption coefficient (0.1, assumes an oxidized surface and high temperatures).

D. ARHOM = Liquid melt absorption coefficient (0.1).

DEBRIS MODULE INPUT

The DEBRIS module input allows the user to control the model through the formation, meltdown, and existence of the calculation.

67. LDBRIS

A. LDBRIS = DEBRIS module calculation switch (0=off, 1=on).

68. NZMAX, NBEDM, ICOND

A. NZMAX = Maximum number of nodes in a bed (40-60).

B. NBEDM = Maximum number of beds.

C. ICOND = Effective conductivity model indicator.

a. ICOND = 1, The Imura-Takegoshi—Vortmeyer model is used.

b. ICOND = 2, The Willhite-Kunii-Smith—Luikov model is used.

69. ALFDBM, PORMAX, DZMIN, DEFF, SO

A. ALFDBM = Minimum melt fraction in a cell to initiate the DEBRIS module (0.60).

B. PORMAX = Maximum allowable porosity (void fraction) in a bed (0.55). If a cell in the bed becomes more porous than this value, the code collapses the cell above into it.

C. DZMIN = Minimum DEBRIS module cell mesh size (0.05 m).

D. DEFF = Effective particle diameter in the bed (0.10 m).

E. SO = Specific power (W/kg). This should first be set to the total initial power divided by the total mass of UO_2. The user should then reduce this value by approximately 20% to account for the release of the volatile fission products.

EXTERNAL DISTRIBUTION:

U.S. Nuclear Regulatory Commission (5)
Division of Reactor System Safety
Office of Nuclear Regulatory Research
ATTN: C. G. Gingrich, T-10K8
S. Basu, T-10K8
Washington, DC 20555-0001

U.S. Department of Energy
Scientific and Technical Information Center
Post Office Box 62
Oak Ridge, TN 37831

Brookhaven National Laboratory
ATTN: R. Bari
Building 130
32 Lewis
Upton, NY 11973

Energy Research, Inc.
ATTN: M. Khatib-Rahbar
Post Office Box 2034
Rockville, MD 20852

Fauske & Associates, Inc.
ATTN: R. Henry
16W070 West 83rd Street
Burr Ridge, IL 60952

Dr. Thomas S. Kress
102-B Newridge Road
Oak Ridge, TN 37830

Massachusetts Institute of Technology
ATTN: M. Golay
Cambridge, MA 02139

Rennselaer Polytechnic Institute
Department of Nuclear Engineering &
Engineering Sciences
ATTN: M. Podowski
Tibbits Avenue, NES Building
Troy, NY 12180-3590

University of California
Department of Chemical and
Nuclear Engineering
ATTN: T. Theofanous
Santa Barbara, CA 93106

University of Wisconsin (2)
Department of Nuclear Engineering
ATTN: M. L. Corradini
J. Murphy
153 Engineering Research Building
1500 Johnson Drive
Madison, WI 53706

FOREIGN DISTRIBUTION:

AEA Technology
ATTN: B. D. Turland
Winfrith, Dorchester
Dorset DT2 8DH
United Kingdom

Autoridad Regulatoria Nuclear
ATTN: J. Baron
Ayacucho 666
5500 Mendoza
Argentina

CEA
C.E.N.G./S.T.I.
ATTN: G. Berthoud
17, rue des Martyrs
38054 Grenoble Cedex 9
France

CEC Joint Research Centre, Ispra
ATTN: D. A. Magallon
TP 421
I-21020 Ispra (Varese)
Italy

Commissariat a l'Energie Atomique
ATTN: M. Petit
Boite Postale No. 6
F-92265 Fontenay-aux-Roses Cedex
France

Forschungszentrum Karlsruhe (2)
ATTN: W. Scholtyssek
H. Jacobs
Post Office Box 3640
75 Karlsruhe, D-76021
GERMANY

Gesellschaft fur Anlagen-und Reaktor
(GRS) mbH
ATTN: M. Sonnenkalb
Schertnergasse 1
50667 Cologne
Germany

Health/Safety Exec. Nuclear Instal. Insp.
ATTN: A. Hall
St. Peter's House, Balliol Rd.
Bootle, Merseyside L20 3LZ
United Kingdom

IAEA
Division of Nuclear Reactor Safety
ATTN: M. Jankowski
Wagranerstrasse 5
Post Office Box 100
A/1400 Vienna
AUSTRIA

Institute for Electric Power Research
Division of Nuclear & Power Engineering
ATTN: Z. Techy
P.O. Box 80
H-1251 Budapest
Hungary

Institute of Nuclear Energy Research
Nuclear Engineering Division
ATTN: S. J. Wang
1000 Wenhua Rd. Chiaan Village
P.O. Box 3
Lungtan
Taiwan 325, Republic of China

Institut Jozef Stefan
Reactor Engineering Dept.
ATTN: B. Mavko
P.O. Box 100
61111 Ljubljana
Slovenia

Japan Atomic Energy Research Institute
Department of Fuel Safety Research
ATTN: K. Hashimoto
Tokai-mura, Naka-gun
Ibaraki-ken, 319-11
Japan

Korea Atomic Energy Research Institute
ATTN: Hee-Dong Kim
150 Dukjin-dong, Yusong-ku
Taejon 305-353
KOREA

Korea Institute of Nuclear Safety
Safety Review and Assess. Div.
ATTN: J. I. Lee
P.O. Box 114, Yusong
Taejon, 305-600
Korea

Netherlands Energy Research Foundation, ECN
Unit Nuclear Energy
Safety & Reliability Engineering
ATTN: R. Jansma
P.O. Box 1
NL-1755 ZG Petten
The Netherlands

Nuclear Fission Energy Sector
ENEA
ATTN: M. Pezzilli
C.R. Casaccia, Via Anguillarese, 301
00060 S. Maria de Galeria (Rome)
Italy

Nuclear Power Engineering Corp.
Advanced Simulation Systems Dept.
ATTN: M. Naitoh
Fujita Kanko Toranomon Bldg. 7F, 17-1
3-Chome Toranomon, Minato-Ku
Tokyo 105, Japan

Nuclear Research Institute Rez plc
ATTN: J. Duspiva
250 68 Rez
Czech Republic

Nuclear Regulatory Council of Spain
ATTN: A. Alonso
Consejo de Seguridad Nuclear
Justo Dorado, II
28040 Madrid
Spain

Royal Institute of Technology
Nuclear Power Safety
ATTN: B. R. Sehgal
S-100 44 Stockholm
SWEDEN

Russian Academy of Sciences
Nuclear Safety Institute
ATTN: V. F. Strizhov
52, B. Tulskaya
113191 Moscow
RUSSIA

South Africa Council for Nuclear Safety
Quantitative Risk Assess. & Compl. Dept.
ATTN: T. Hill
P.O. Box 7106
Hennopsmeer 0046
Republic of South Africa

Swedish Nuclear Power Inspectorate
ATTN: W. Frid
Post Office Box 27106
S-102 52 Stockholm
SWEDEN

TracteBel
Operation & Accident Analysis Section
ATTN: M. Auglaire
Avenue Ariane 7
B-1200 Brussels
Belgium

University of Sydney
Dept. of Chemical Engineering
ATTN: D.F. Fletcher
NSW 2006, Australia

VTT Energy
ATTN: R. Sairanen
Leader of Accident Management Group
Tekniikantie 4 C, Espoo-Otaniemi
P.O. Box 1604, FIN-02044 VTT
Finland

INTERNAL DISTRIBUTION:

MS0619	Review & Approval Desk, 00111 (1) For DOE/OSTI
MS0736	D. A. Powers (6400)
MS0739	K. D. Bergeron (6421) (5)
MS0739	M. F. Young (6421) (5)
MS0742	J. R. Guth (6414)
MS0899	Technical Library, 4916 (2)
MS1139	M. M. Pilch (6423)
MS1139	K. O. Reil (6423)
MS9018	Central Technical Files (8940-2)